Experimental Thermal and Fluid Science 34 (2010) 879–892

Contents lists available at ScienceDirect

Experimental Thermal and Fluid Science

journal homepage: www.elsevier.com/locate/etfs

Experimental investigations on flashing-induced instabilities in one and two-parallel channels: A comparative study

Christian P. Marcel *, M. Rohde, T.H.J.J. Van Der Hagen

Department of Physics of Nuclear Reactors, Delft University of Technology (TUDelft), Delft 2629 JB, The Netherlands

ARTICLE INFO

Article history:
Received 2 September 2009
Received in revised form 29 January 2010
Accepted 4 February 2010

Keywords:
Parallel channels
Flashing-induced instabilities
Natural circulation

ABSTRACT

In this investigation, experiments conducted in a natural circulation test facility at low power and low pressure conditions, in the one single and two-parallel channels configuration are presented and discussed in detail. The novel manner of visualizing the results allowed characterizing the facility at any time and position which helped to thoroughly understand the instability mechanisms. Different modes were observed for each configuration. In the case of having two-parallel channels, four different behaviors have been observed: stable flow circulation, periodic high subcooling oscillations, a-periodical oscillations and out-of-phase periodical oscillations. In addition, stability maps were constructed in order to clarify the region in which each mode is dominant. The results obtained from both the one and two-parallel channels configurations are thus analyzed and compared. As a result, some similarities have been observed between the intermittent flow oscillations found in the single channel experiments and the high subcooling oscillations found in the two-parallel channels experiments. Moreover, similarities have also been found between the sinusoidal flow oscillations existing in the single channel experiments and the out-of-phase oscillations from the two-parallel channels experiments. The experiments presented in this work can be used to benchmark numerical codes and modeling techniques developed to study the start-up of natural circulation BWRs.

1. Introduction

Natural circulation cooling is a key issue in the design of modern nuclear power plants for simplicity, inherent safety, and maintenance reduction features [21]. For this reason, new generation boiling water reactors (BWRs), which are optimized to be economical and reliable, are cooled with natural circulation in order to improve their competitiveness. The prototypical natural circulation BWR (NCBWR) is the Economic Simplified Boiling Water Reactor (ESBWR) [4,22]. An item of concern of these reactors is the susceptibility to exhibit thermal–hydraulic instabilities since the flow cannot be controlled externally as in forced circulation systems.

Safety concerns of nuclear reactors have attracted the attention of many researchers on flow instabilities in natural circulation boiling loops. Experiments performed on the DANTON facility at start-up conditions (i.e. low pressure-low power) have shown that the pressure increase caused by the steam produced in the reactor vessel is not sufficient to suppress completely the flow oscillations and that without external pressurization, an instability region between single-phase and two-phase operation has necessarily to be crossed [23]. Unstable behavior at low power and low pressure has also been encountered at specific conditions explored in an experimental campaign at the Dutch natural circulation BWR Dodewaard [26,27].

The tall adiabatic chimney, placed on top of the core to enhance the flow circulation, makes flashing phenomenon (the sudden increase of vapor generation due to the reduction in hydrostatic head) likely to occur during the low pressure start-up phase of NCBWRs. The feedback between vapor generation in the chimney and buoyancy in the natural-circulation loop may give rise to self-sustained flow oscillations.

Flashing-induced flow oscillations were first pointed out by the pioneering work of Wissler and colleagues [25], who reported about flashing-induced instabilities in a natural circulation steam/water loop in the 1950s. Since then, several experimental studies have addressed stability of natural circulation two-phase flow systems at low pressure [1,12,13,14,23,15].

These flow oscillations make the operation of the reactor during start-up rather difficult and could cause strong mechanical vibrations of the reactor's internal components. Well-defined start-up procedures are therefore needed to cross the instability region during the transition from single-phase to two-phase flow conditions.

* Corresponding author. Present address: Centro Atómico Bariloche; Av. E. Bustillo km 9.5 (8400), S.C. de Bariloche, Río Negro, Argentina. Phone: +54 2944 445100x5384.
E-mail addresses: christian.marcel@cab.cnea.gov.ar, chris.p.marcel@gmail.com (C.P. Marcel).

0894-1777/$ - see front matter © 2010 Elsevier Inc. All rights reserved.
doi:10.1016/j.expthermflusci.2010.02.002

Nomenclature

A	section flow area
Cp_l	specific heat capacity at constant pressure
D	section diameter
E^*_{kin}	kinetic energy per unit of volume
M	inlet mass flow rate
F^*_{driv}	two-phase driving force per unit of area
g	acceleration due to gravity
K_{in}	inlet friction coefficient
L	section length
q	applied power
Q	time averaged coolant volumetric flow rate
t	cross correlation time delay
u_{in}	coolant mean inlet velocity
v_{gj}	drift velocity
V	volume of the section and

Greek letters

α	void fraction
ΔP	inlet restriction pressure drop
$\Delta T_{sub,in}$	fluid subcooling at the channel inlet
$\Delta\rho$	density difference between liquid and vapor phases
ρ_l	coolant inlet density
τ	transfer function from void-fraction fluctuations to flow rate time constant
$\tau_{Channel}$	fluid transit time in the channel
τ_{bd}	boiling delay time
τ_f	period of geysering-induced oscillations
$\tau_{b,tt}$	transit time of the bubbles passing through the chimney

Subscript

0	relative to the steady state condition
C	relative to the heated section
Ch	relative to the chimney section
$Channel$	relative to the channel
DC	relative to the downcomer
l	relative to the liquid phase
$model$	referred to model
v	relative to the vapor phase

Operators

$\langle\ \rangle$	time average

Marcel et al. [17] performed a thoroughly description of the mechanism of flashing-induced oscillations occurring in the CIRCUS test facility with a single chimney configuration. The experiments were presented in a novel manner, allowing observing the dynamic evolution of important parameters which gave an excellent characterization of the phenomenology present in the system.

In natural circulation BWRs the chimney section is usually divided into subchannels to avoid cross flow and to better divide the coolant flowing through the core. Flashing-induced instabilities occurring in parallel channels may occur during the start-up phase of a natural circulation BWR equipped with such adiabatic sections. Such instabilities may be different from the more common flashing-induced oscillations occurring when only one chimney is present. Experimental investigations on this field are still very limited. Aritomi et al. [1,2] studied the low pressure stability of parallel channels with a chimney but in their experiments, the chimneys were too short compared to those from modern natural circulation BWRs, and therefore flashing played a secondary role. Fukuda and Kobori [11] observed two modes of oscillations in a natural-circulation loop with parallel heated channels. One was the U-tube oscillation characterized by channel flows oscillating with 180° phase difference, and the other was the in-phase mode oscillations in which the channel flow oscillated along with the whole loop without any phase lag among them. Out-of-phase oscillations were also observed in the parallel channels of the CIRCUS facility by Marcel et al. [16]. The mechanism of flashing-induced instabilities occurring in two-parallel channels, however, is not fully understood and therefore, more experimental investigations are needed in order to clarify this issue. Such a topic is important to assure a safe start-up process of novel natural circulation BWRs.

2. Investigation tools

2.1. The CIRCUS facility in the single channel configuration

The CIRCUS facility [9] is a steam/water facility designed to perform studies on two-phase flow dynamics relevant for the starting-up of natural circulation BWRs. CIRCUS is an axially fully scaled, radially lumped version of the Dodewaard reactor [26] . A simplified scheme of the CIRCUS facility including technical details is given in Fig. 1. Further details regarding the CIRCUS facility (e.g. location of sensors, geometry, etc.) can be found in Appendix A.

CIRCUS can be operated in two different ways: the single chimney configuration and the two parallel chimneys configuration. In the first one, CIRCUS is equipped with a single tall adiabatic section representing the reactor chimney which is placed on top of the heated section. The heated section simulates the reactor core and consists of two heated channels with two bypasses. For this reason this section is also referred as the 'core' section.

The steam produced in the heated section and in the chimney is condensed in the heat exchangers and to some extent in the steam dome. A buffer vessel is used to damp temperature oscillations at the downcomer inlet, ensuring a constant inlet subcooling. Two magnetic flow-meters (maximum inaccuracy of ±0.01 l/s) characterize the flow at the heated section inlet and chimney outlet. Several thermocouples (maximum inaccuracy of ±0.5 °C) are located at the inlet and outlet of each heated channel, along the chimney sections, in the heat exchanger and in the steam dome. Two PT100 sensors are located at the inlet of the core section and in the steam dome for more accurate temperature measurements. Absolute pressure sensors are placed at the inlet of the core section, at the chimney outlet and in the steam dome. Differential pressure sensors are mounted across the steam dome, for measuring the water level, and across the core inlet valve. Advanced measuring techniques are used for detailed high sampling rate void-fraction measurements, e.g. conductivity needle probes and capacitance-based sensors. The channels in the facility are made of glass, allowing visual inspection during the operation. To reduce the heat losses to the surroundings, all the sections are covered with removable thermal isolation.

CIRCUS can be operated with a maximum electrical power per rod of 3 kW. By varying the inlet subcooling and the applied power, several configurations can be studied in the power-subcooling plane. The core inlet valve allows changing the inlet restriction coefficient.

2.2. The CIRCUS facility in the two-parallel channels configuration

In this configuration, the CIRCUS test facility is operated with two chimneys on top of the core section (see Fig. 1).

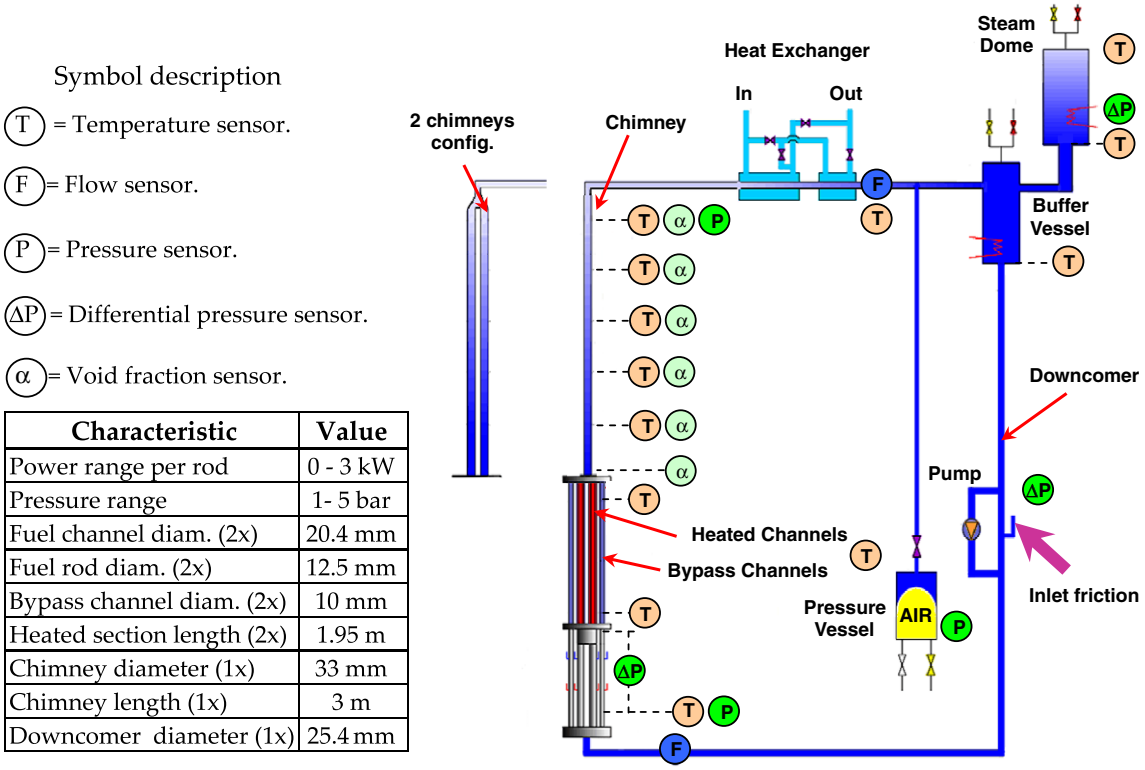

Characteristic	Value
Power range per rod	0 - 3 kW
Pressure range	1- 5 bar
Fuel channel diam. (2x)	20.4 mm
Fuel rod diam. (2x)	12.5 mm
Bypass channel diam. (2x)	10 mm
Heated section length (2x)	1.95 m
Chimney diameter (1x)	33 mm
Chimney length (1x)	3 m
Downcomer diameter (1x)	25.4 mm

Fig. 1. Schematic view of the CIRCUS facility and its sensors in the single chimney and the two-chimney configuration (not to scale).

Two parallel chimneys are installed above the four electrically heated channels representing the core, from which two of these are connected to each chimney. *Channel 1* represents the set of heated channels number 1 and 2 together with Chimney 1; *Channel 2* represents the set of heated Channels 3 and 4 together with Chimney 2. In this configuration, the CIRCUS facility is equipped with 16 void sensors for measuring the axial void-fraction profile in the chimneys. Moreover, 30 thermocouples allow measuring the temperature in the loop. Reverse flow (counter-current flow) may occur in the channels during very strong oscillations. Special high sensitive dp-sensors capable of measuring both negative and positive pressure drops are therefore installed at the inlet of each heated channel and core bypass channels where the coolant is always in liquid phase for all conditions.

3. Experimental results

The following experiments are performed with the steam dome open to the surroundings, thus the pressure at the top of the facility is assumed to be always at 1 bar. In this way, any pressure feedback occurring during oscillations is greatly reduced. Each experimental point is obtained by fixing the power applied in the heating rods and varying the inlet temperature by changing the power applied in the buffer vessel. By repeating this process at different powers, the whole operational map can be covered. The operational conditions used for the experimental study performed in the CIRCUS facility are summarized in the following table (see Table 1).

The value of the inlet friction coefficient is obtained experimentally by taking the channel flow area A_C as a reference.

The inlet subcooling is defined in terms of the saturation temperature at the steam dome (100 °C).

In this investigation, the same friction has been used for the single channel and the two-parallel channels configuration, which corresponds to $K_{in} = 5.6$.

Table 1
Experimental conditions for the measurements obtained with CIRCUS facility in the single chimney configuration.

Magnitude	Value
Power per rod	0–3000 W
Inlet temperature	50–99 °C
Pressure	1 bar
Flow circulation	Natural
Core-bypass channels	Closed
Number of chimneys	1
Inlet restriction coef.	5.6

3.1. Single channel configuration

3.1.1. The stability maps

Fig. 2 shows the stability map corresponding to the single channel configuration.

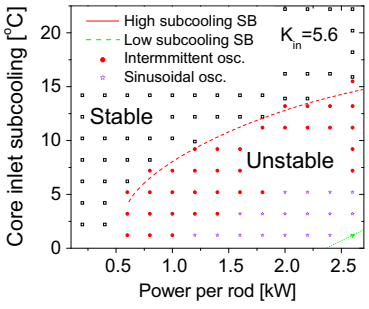

Fig. 2. Measured stability boundaries corresponding to the case with $K_{in} = 5.6$.

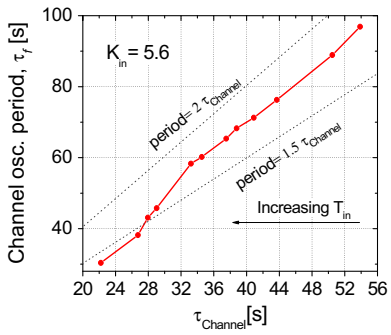

Fig. 3. Channel oscillation period vs. transit time for the case with K_{in} = 5.6.

The power-subcooling plane is useful to characterize the system since with these two parameters the working point of the facility is univocally determined.

From the results it is observed that instability occurs within a certain range of inlet subcooling. This result is in agreement with findings reported in literature (see [12,15,18]).

In order to clarify the origin of the instabilities the period of experimental oscillations is compared with typical periods of DWOs. The fluid transit time in the channel is estimated as

$$\tau_{Channel} = \frac{V_{Ch} + \frac{1}{2}V_C}{Q}, \quad (1)$$

where Q is the time averaged coolant volumetric flow rate, V_{Ch} the volume of the chimney section and V_C the total volume of the core section. The factor 1/2 before V_C appears since a perturbation of the inlet flow rate produces a perturbation of the enthalpy at the core outlet with an average phase lag corresponding to half of the transit time from the inlet to the outlet of this section. Since the transit time is a time-dependent variable in case of flow oscillations, it is evaluated on the basis of the mean flow rate.

Oscillatory cases obtained by applying 2 kW per rod have been selected for this investigation. The relation between the oscillation period and the transit time for such experimental cases is shown in Fig. 3.

The oscillation period from the experiments agrees well with the estimated one from DWOs (being between one-and-a-half to two times the coolant transit time through the channel) indicating the density wave character of the flashing-induced oscillations. It has to be recalled that numerical simulations performed by Manera [15] have shown that the strong effect of the energy accumulated in the heat structures, namely the chimney walls and heated section tends to increase the incubation time and therefore the oscillation period. Heat losses have shown to cause the same effect. Such phenomena are obviously present in the results presented here. For small oscillation periods, which correspond to low subcooling values, the period slightly deviates from these limits. In order to understand this, a more detailed characterization of the experiments is needed. Such a study is presented in the following section.

3.1.2. From stable to unstable

From experiments such as those presented in Fig. 2 it is observed that by increasing the inlet temperature (while maintaining the power constant) four different types of behavior are present [15]: (a) stable flow at high subcooling, (b) unstable *intermittent* two-phase flow, (c) unstable *sinusoidal* two-phase flow, and (d) stable flow at low subcooling. These four behaviors have been extensively discussed in [17]. Part of that analysis is included here in order to discus similarities and differences with the results obtained with the two-parallel channels configuration. The experiments selected here correspond to K_{in} = 5.6, a power of 2 kW per rod and different inlet subcoolings. It has to be noted that for this configuration, the behavior with stable flow at low subcooling could not be reached.

To characterize the facility at any position and time, the temporal evolution of the axial temperature profile in the channel together with the void fraction axial profile in the chimney is included in special plots developed for that purpose. In these plots the color scale represents the value of the corresponding variable while the horizontal and vertical axes refer to the time and the axial position, respectively. The temperature profile is obtained from the eight different places where the temperature is measured (see Fig. 1). The void fraction evolution is reconstructed from the six void sensors placed in the chimney. A small scheme of the CIRCUS facility is included to clarify the axial positions in the plots.

Time traces of the core inlet coolant flow are plotted together with the power spectral decomposition (PSD).

3.1.3. High subcooling stable flow circulation

Fig. 4 presents the case measured with an inlet temperature of 86 °C, where single-phase buoyancy plays a major role.

It is seen that cold water enters the channel and is heated in the core section. The coolant then travels through the chimney section with no significant heat losses.

The temperature profile and the flow remain unchanged in time, only exhibiting small fluctuations which can be attributed to statistical fluctuations and turbulence. This is in accordance with the PSD plot of the flow signal where no natural frequency is seen. In this case, no significant amount of vapor is detected in the chimney (see void fraction plot).

3.1.4. Intermittent oscillations

By reducing the coolant inlet subcooling the high subcooling stability boundary is crossed where intermittent oscillations are found. Fig. 5 shows the case with an inlet temperature of 89.2 °C.

In order to clarify the details of the dynamic process shown in the plots, let us focus on what happens at ~30 s. The coolant is heated in the core, driving the flow upwards due to single-phase natural circulation (no vapor is identified in the chimney). At a certain point flashing occurs in the chimney since the saturation temperature is reached by the hot coolant.

The vapor created by flashing enhances the flow circulation. Due to the flow increase, the coolant passes the heated section faster and therefore is heated less. This liquid bulk is not hot enough to vaporize in the chimney and flashing thus stops. As result of this, the driving mechanism is again single-phase buoyancy and the flow circulation decreases. This flow decrease causes the coolant to stay longer in the heated section and consequently the temperature at the chimney inlet starts to increase. Some vapor is consequently created by boiling at regions close to the core exit, causing a small second flow increase which disappears soon after entering the chimney. The hot front originated in the heated section travels upwards starting the cycle again. Since from one flashing event to the next one a certain time is needed (the so-called incubation time) this behavior is named intermittent flashing.

As in the experiments with the single chimney configuration, the interaction with the structures (in particular in the chimneys) and the heat losses most probably influences the incubation time of the system.

The PSD plot shows numerous frequencies after the main frequency indicating the presence of higher modes.

3.1.5. Sinusoidal oscillations

A further decrease in the inlet subcooling allows reaching the unstable case with sinusoidal oscillations. The results of the measurements performed with an inlet temperature of 95.1 °C are depicted in Fig. 6.

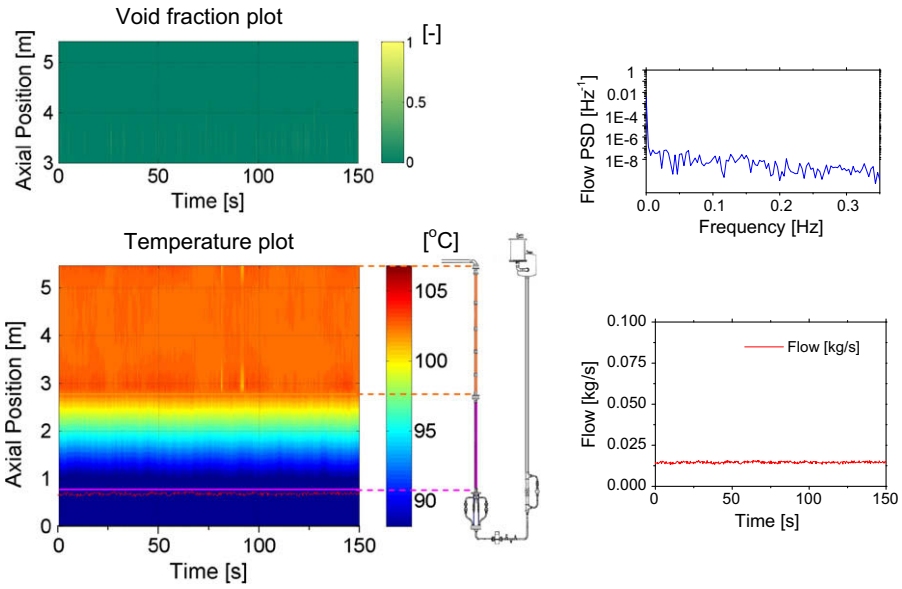

Fig. 4. Stable high subcooling flow circulation. Very low vapor values and a constant axial temperature profile in the chimney characterize this case. The flow signal is roughly constant only exhibiting some noise.

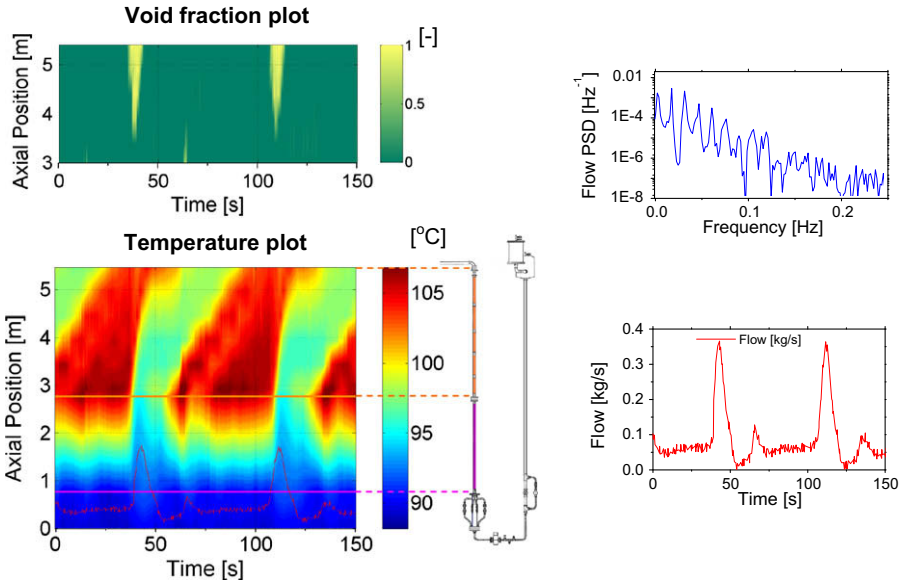

Fig. 5. Unstable *intermittent* oscillations. This case is characterized by periodical oscillations occurring after a certain incubation time. The PSD plot shows clear frequencies.

Unlike the intermittent oscillations case, in the sinusoidal oscillations case during the flashing event vapor appears in the core section first. The coolant flow shows a regular behavior with a non-existent incubation time (see the PSD plot).

It is seen that just before the steam is produced in the core, the temperature profile shows a clear hot spot (see Fig. 6). It is expected that the existing negative temperature gradient (Including the heat transfer with the structures) may diminish the vapor creation. An extreme example of this effect is the geysering phenomenon which can lead to sustainable oscillations. Since the geysering mechanism is characterized by a much longer oscillation period than that of DWOs, having such temperature profile prior to the flashing event may tend to reduce the oscillation period. This agrees with the shorter oscillation periods found for the cases with low subcooling values (see Fig. 3).

3.1.6. Low subcooling stable flow circulation

By increasing the coolant temperature at the core inlet even further, the low subcooling stable case is found (see, for example Fig. 8 from [17]).

In this case, coolant in a two-phase state is permanently present in the chimney. The temperature profile is characterized by a clear temperature decrease in the flashing region. This decrease is due to the decrease in the saturation enthalpy which corresponds to the hydrostatic pressure decrease.

3.1.7. Analysis of the dynamics of the flashing front

In this section, the dynamics of the flashing front for the two oscillatory cases is further investigated. The signals from the non-intrusive, high frequency, capacitance-based void detectors are used for this purpose.

The cases presented in Figs. 5 and 6 are used in this section. The time traces of the signals from the void fraction sensors placed in the chimney are shown in Fig. 7a. To facilitate the comprehension, the sensor positions are numbered from bottom to top, being the lowest one number "1" and the top one number "6".

Fig. 8a shows that in the intermittent oscillations case the flashing front starts at the top of the chimney, at positions 6 and 5. This is due to the fact the temperature profile is quite flat prior to the onset of flashing (see Fig. 5) and therefore flashing is likely to occur at higher positions where the hydrostatic pressure is lower. The flashing front then reaches the lower regions in the chimney, at positions 4 and 3. The flashing front then travels upwards leaving the chimney.

The flashing front evolution for the sinusoidal two-phase oscillatory case is presented in Fig. 7b. As can be observed, in this case vapor appears at the lowest void sensor location first and then travels upwards along the chimney.

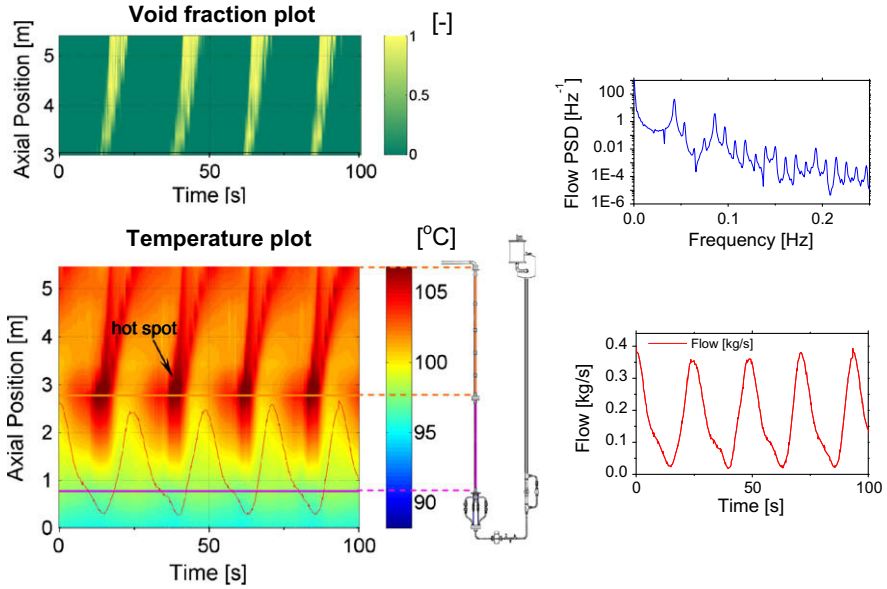

Fig. 6. Sinusoidal oscillations case. This behavior is characterized by regular oscillations with a practically non-existent incubation time. The flashing/boiling front starts inside the heated section.

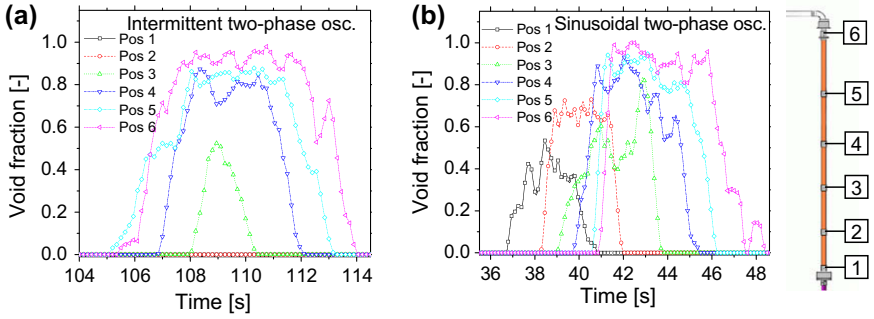

Fig. 7. (a) Time evolution of the flashing front for the intermittent oscillations and (b) flashing front time evolution for the sinusoidal oscillatory case.

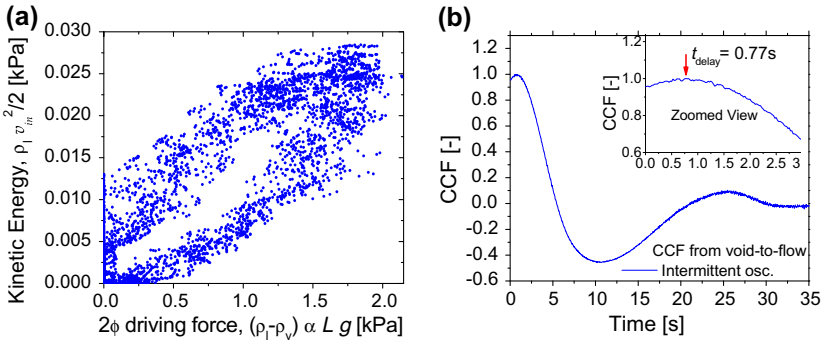

Fig. 8. (a) Relation between the driving force and the kinetic energy. (b) Cross correlation between the void fraction and resulting flow response.

3.1.8. Analysis of the inertia of the loop

During the oscillations the buoyancy in the system is mainly due to the two-phase driving force which, per unit of area, is defined as follows

$$F^*_{driv} = (\rho_l - \rho_v)\alpha\, L\, g, \tag{2}$$

where α is the mean void fraction (obtained by integrating in space the temporal evolution of the axial void fraction in the channel) and L is the channel length. The use of fast response void fraction and pressure drop sensors assure that no dynamic effects are introduced by the measurement system (besides some delay which may be introduced by the void transport).

The system response due to a change in the driving force can be accounted by the kinetic energy per unit of volume, which is defined as

$$E^*_{kin} = \rho_l u^2_{in}/2, \tag{3}$$

where v_{in} is the coolant velocity at the core inlet.

Fig. 8a illustrates the response of the kinetic energy to changes in the two-phase driving force, for intermittent oscillations measured with $K_{in} = 5.6$ an inlet temperature of 88 °C and a power input of 2 kW per rod.

The figure clearly shows that no linear relation exists between the two plotted quantities. To clarify this issue, the cross correlation of the mean void fraction and the coolant velocity is calculated and plotted in Fig. 8b.

A clear time delay of ~0.77 s exists between these two signals. The time constant of the transfer function from void-fraction fluctuations to flow rate can be estimated from a first-order transfer function derived from a model based on the linearized version of the momentum balance (see [18] in which two driving mechanisms are considered: the single-phase and the two-phase natural circulation.

$$\tau = \frac{M_0 \sum_i \frac{L_i}{A_i}}{2L\, g[\langle\alpha\rangle_{Ch}(\rho_{l,Ch} - \rho_v) + (\rho_{l,DC} - \rho_{l,Ch})]}. \tag{4}$$

A time constant of τ_{model}= 0.91 s is found from the model, which is in the same range as the time delay from the cross correlation (t_{delay} = 0.77 s). The inertia term $\Sigma l_i/A_i$ is particularly important in natural circulation systems and therefore has to be taken into account. In other words, the flow cannot be considered to instantaneously adjust itself to changes in driving force and friction.

It can be concluded that the delay between the two-phase driving force and the kinetic energy is caused by a combination of two effects: the inertial effects of the fluid plus some delay which may be introduced by the void transport.

Table 2
Experimental conditions corresponding to the measurements performed in the CIRCUS facility with parallel channels.

Magnitude	Value
Power per rod	0–3000 W
Inlet temperature	70–99 °C
Pressure	1 bar
Flow circulation	Natural
Core-bypass channels	Closed
Number of chimneys	2
Inlet restriction coef.	5.6

3.2. Two-parallel channels configuration

As in the case with only one chimney, during the experiments with the two-parallel channels configuration, the power applied in the heating rods is fixed and the inlet temperature is varied by changing the electrical power applied in the buffer vessel. By repeating this procedure with different powers, the full operational map can be covered. The operational conditions used in this study are summarized in Table 2.

3.2.1. The stability maps

In the out-of-phase oscillation mode, the primary flow remains constant, i.e. the total pressure drop in the parallel channels remains the same. Such oscillatory behavior, however, is never observed in our experiments. As soon as the system loses stability, the primary flow exhibited oscillations.

Fig. 9 shows the stability map found when K_{in} = 5.6 is set. The stability map is divided into four regions, each one characterizing a different behavior for which typical time traces of the primary flow are also included in the figure.

The first region I is mainly characterized by stable single-phase flow. In the proximity of the stability boundary small bubbles were

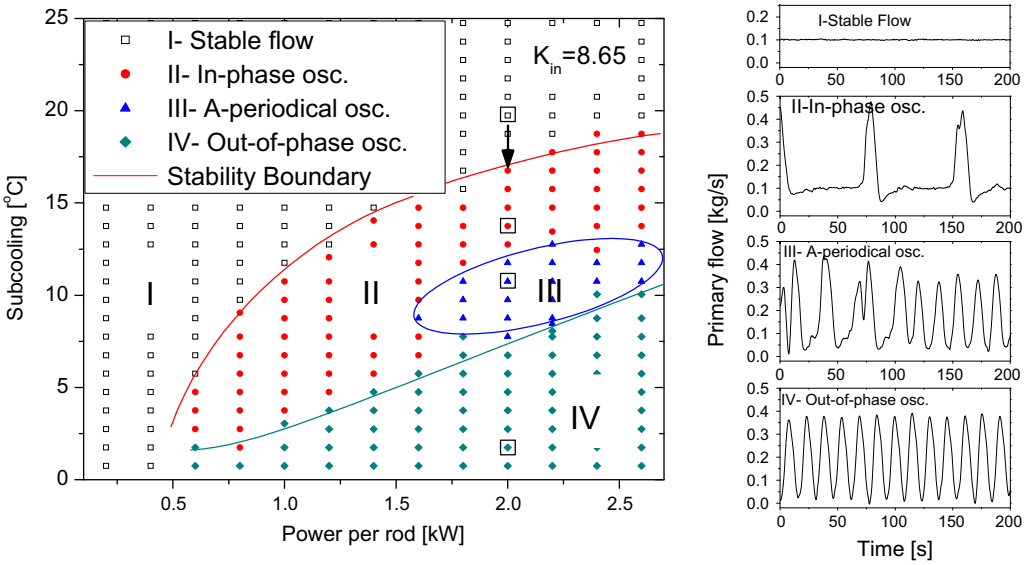

Fig. 9. Stability map and typical time traces of the flow found when the inlet friction is set to a value equal to K_{in} = 5.6. The experiments marked with a '□' are analyzed in detail in Sections 3.2.3–3.2.6. The arrow indicates the points used in the investigation presented in Section 3.2.7.

observed at the chimney exit corresponding to low vapor quality values.

The high subcooling oscillations are observed in region II. This region exhibits regular oscillations in which the period and time of occurrence of the cycles is the same for both the channel partial flows and the primary flow.

In region III, so-called a-periodical oscillations take place in the system.

In the last region IV regular oscillations, which are out-of-phase regarding the partial flow in the channels, are found.

A more detailed description of the four behaviors is provided in next sections. It has to be remarked that no stable flashing region is observed in this set of measurements.

3.2.2. Phenomenological description – from regions I–IV

To clarify the four behaviors introduced earlier, selected experiments performed with a power input of 2 kW per rod are presented in detail in this section. These cases are marked with '□' in Fig. 9.

The dynamics of the axial temperature profile and the void-fraction profile in the two channels is displayed by using the same technique used before. These profiles are obtained from the sixteen different positions where the temperature and the void fraction is measured (see Fig. 1). Finally, to easily correlate the dynamics of the flow changes with the void and the temperature fluctuations in the channels, the partial flows are also superimposed on the axial temperature plots.

The partial flows time traces are plotted to show the differences between the cases. The primary flow signal power spectral decomposition (PSD) is also shown.

3.2.3. Region I – high subcooling stable flow circulation

A measurement performed with an inlet temperature of 80 °C is selected as example of the stable behavior of region I. Fig. 10 shows this case where stable single-phase natural circulation occurs in the facility.

The temperature profile is similar in both channels. The partial flows only exhibit small fluctuations which can be attributed to statistical fluctuations and turbulence. In this case no natural frequency is observed in the PSD of the primary flow signal.

From the figure it is observed how cold water entering into the channels is heated in the core section. The coolant then travels through the chimney section with no significant heat losses. The main flow circulation driving mechanism is single-phase buoyancy since no significant void is detected.

This behavior is similar to the high subcooling stable flow circulation behavior reported in Section 3.1.3 obtained when having a single chimney.

3.2.4. Region II – unstable high subcooling flow circulation

Fig. 11 shows the typical behavior from region II. This particular case is obtained by operating the facility with an inlet temperature of 87 °C.

Here, flashing occurs almost simultaneously in both chimneys (see the large peaks in the partial flow signals) since the conditions for flashing in both channels are fulfilled practically at the same time. In this region the period and time of occurrence of the oscillations is the same for both partial flows and primary flow. The coupling between the channels cause that during the flashing events the partial flows behave out-of-phase.

In order to clarify the process, let us focus on what happens at ~100 s. As can be seen in Fig. 11, (see plots with vapor), large amounts of vapor are present in Channel 2 while Channel 1 still contains liquid water. Consequently, a strong increase in flow appears in Channel 2 due to buoyancy. As a result, reversed flow occurs in Channel 1 due to the large inertia of the coolant in the downcomer. This reversed flow forces hot coolant to re-enter the core section and triggers the creation of large amounts of vapor in Channel 1. As a consequence, the partial flow in Channel 1 strongly increases, thereby now reversing the flow in Channel 2. Hence, the water present in the core of Channel 2 is also heated twice (similar to Channel 1). The temperature in the lower part

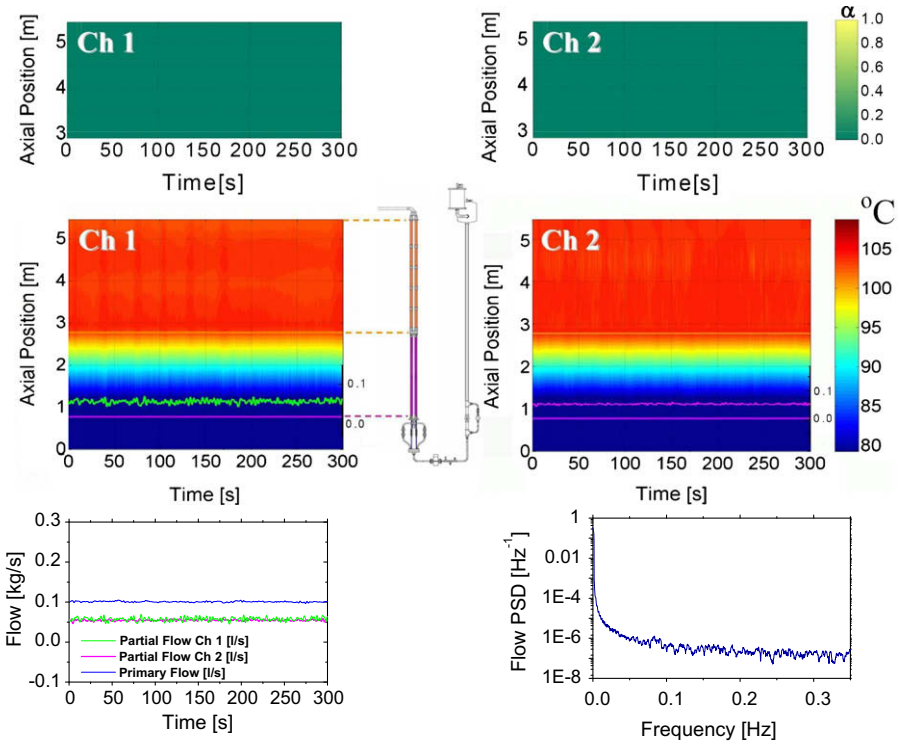

Fig. 10. Region I is characterized by identical axial temperature profiles in the channels and stable flows, similarly to the high subcooling stable cases from Section 3.1.3.

of the chimney in Channel 2 is too low to create vapor now. Some flashing, however, occurs due to the presence of hot coolant at the middle of the chimney in Channel 2. The partial flow in Channel 2 increases for a second time which causes (again) reversed flow in Channel 1. The coolant in Channel 1, however, is now too cold to flash again.

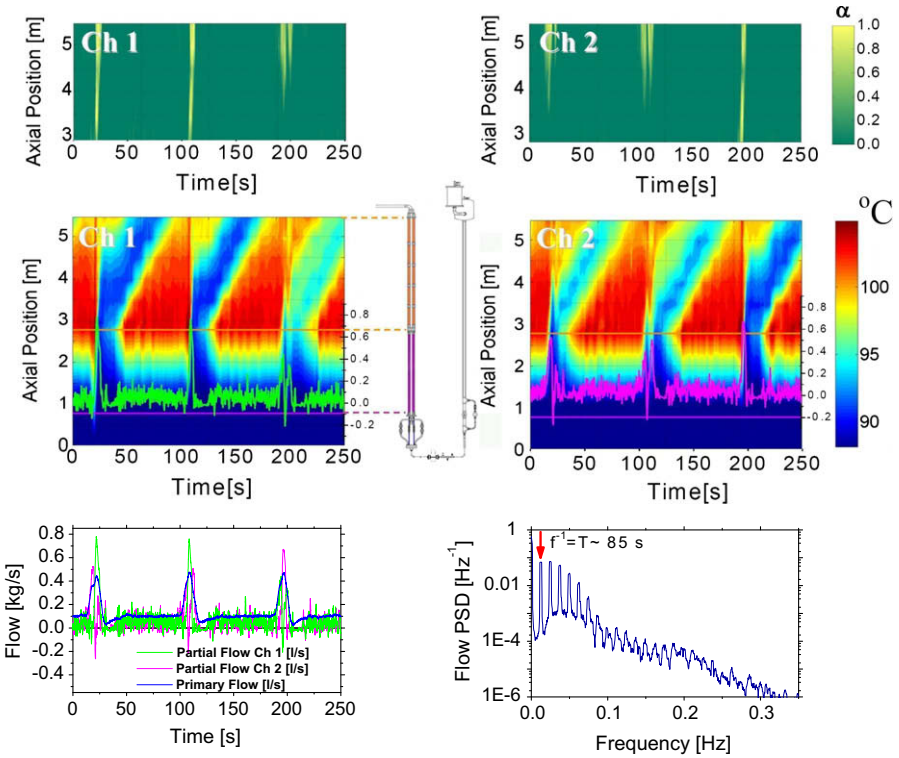

Fig. 11. Region II. The high subcooling oscillations are characterized by showing similar temperature axial profiles in both channels at any time. Large amplitude oscillations take place followed by a relative long incubation time.

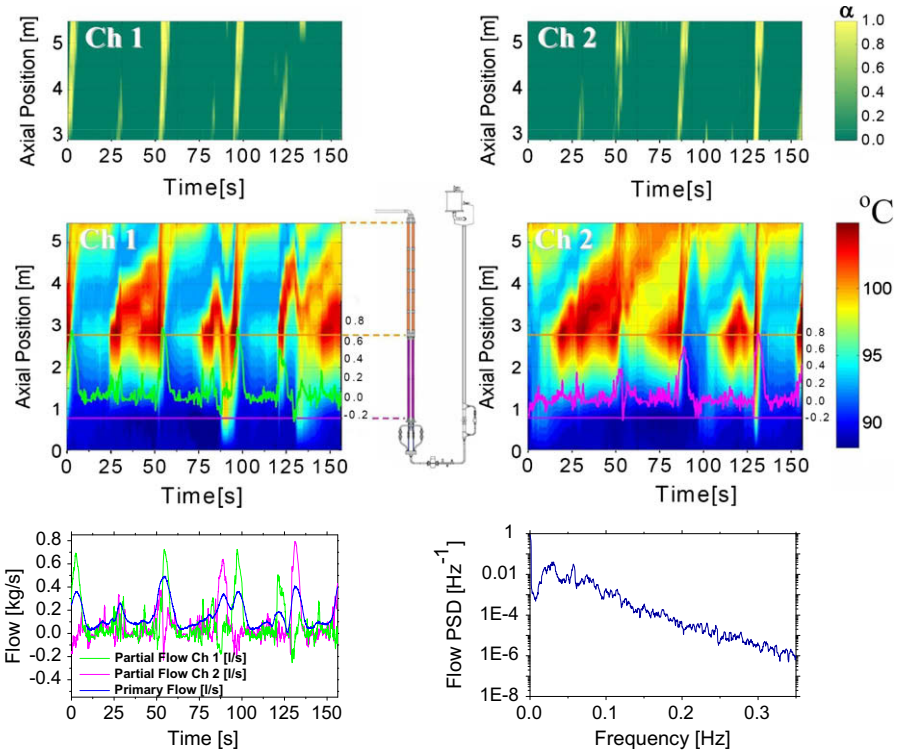

Fig. 12. Region III. The a-periodical oscillations exhibit a very complex temperature and void fraction axial profile in the channels.

To summarize, the parallel channels show reversed flow and flashing in an alternating, but not sustainable way due to the relatively low power and low inlet temperature. Since the channels behave more or less independently (whereas the mutual coupling only triggers the flashing events synchronizing the channels) this behavior can be compared with the intermittent oscillations reported in Section 3.1.4 occurring in a system with a single chimney.

From the analysis of the primary flow signal, two different time scales can be identified: the fast changes in flow (~3 s), caused by the very strong coupling between the channels during flashing, and the long incubation time (~85 s) needed to build up the conditions that will lead to the next flashing cycle in the channels. Numerous frequencies appear in the PSD.

3.2.5. Region III – unstable a-periodical oscillations

A further increase in the inlet temperature leads to the a-periodical oscillations of region III. A typical case of this behavior is shown in Fig. 12, obtained with the inlet temperature set equal to 88.5 °C.

In this case, the combination of power and inlet temperature leads to very complex dynamics resulting in a-periodical oscillations which are clearly visible in the axial void fraction and temperature plots. This behavior is hard to predict, contrasting with the regular oscillations from regions II and IV.

In this region, since the periodicity is lost, a broad range of amplitudes and frequencies is found in the PSD of the primary flow signal which is characterized by the absence of clear peaks.

Despite the complex axial temperature profiles existing in the channels, the correspondence between the presence of void and the increase in flow can still be seen. This a-periodical region is studied in depth in [7].

3.2.6. Region IV – unstable out-of-phase oscillations

Increasing the inlet temperature even more leads to region IV, where so-called out-of-phase regular oscillations are found. The experiment depicted in Fig. 13 is obtained by setting the inlet temperature equal to 98.0 °C.

To better explain the process taking place in this region, we will focus on what happens at ~39 s. The high core inlet temperature causes very hot coolant being present at the exit of the heated section of Channel 1 resulting in large amounts of vapor in the chimney (see void plot in Channel 1), while Channel 2 still contains liquid water. As a result of the vapor appearance in Channel 1, buoyancy abruptly increases the partial flow in this channel. The large increase in the Channel 1 flow causes reversed flow to occur in Channel 2, due to the large inertia of the coolant present in the downcomer. This reversed flow forces hot coolant to re-enter the heated section of Channel 2, where it is heated for the second time.

The combination of high power and inlet temperature causes the alternation of flashing events in both channels to be sustained, in contrast to the cases from region II. Due to the small inlet subcooling, the coolant that is heated twice starts to boil inside the heated sections. The noticeable gradient in the chimney axial temperature profile prior flashing causes condensation that suppresses the vapor creation during the resulting oscillations (see the vapor decrease in the middle part of the flashing chimney).

The time evolution of the void-fraction profile shows a clear correlation in time between the vapor creation and the flow increase in the corresponding channel. It is also found that some vapor produced in one channel enters the other channel due to reversed flow.

The PSD of the primary flow signal exhibits a clear peak at the oscillation frequency and also higher harmonics.

3.2.7. Analysis of the instability mechanism

Since two possible instability mechanisms are identified, flashing and geysering, the periods of the unstable cases obtained when applying a power input of 2 kW per rod (indicated in Fig. 10 with an arrow) are compared with two characteristic parameters of density wave oscillations (DWO) [3,28] and geysering oscillations

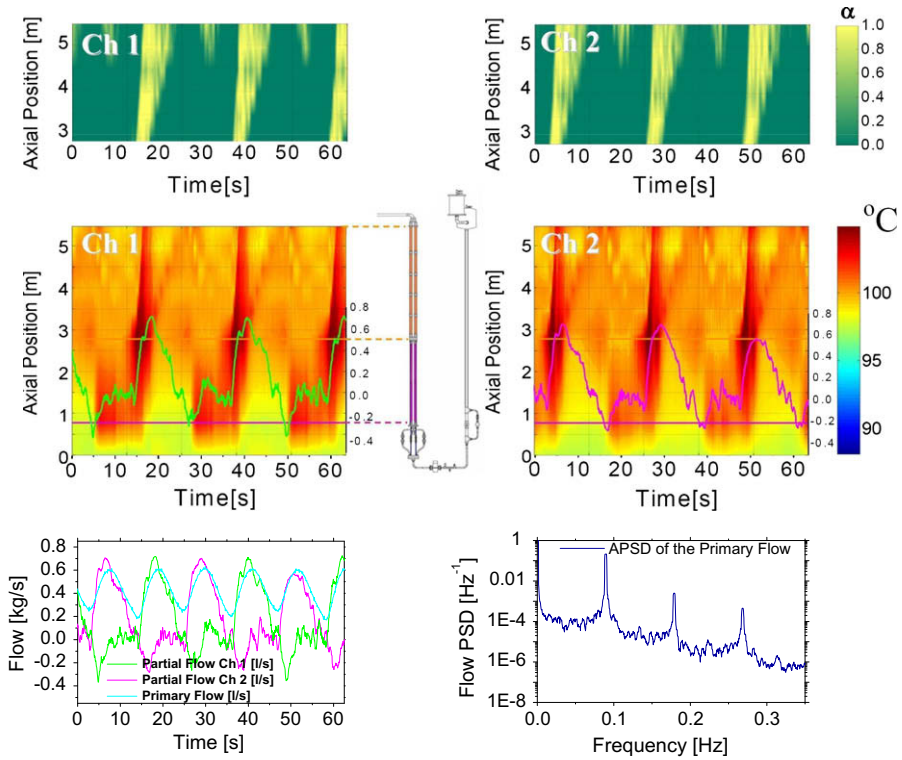

Fig. 13. Region IV. The out-of-phase oscillations are extremely regular, where reverse flow plays an important role creating 'hot spots' which will flash afterwards.

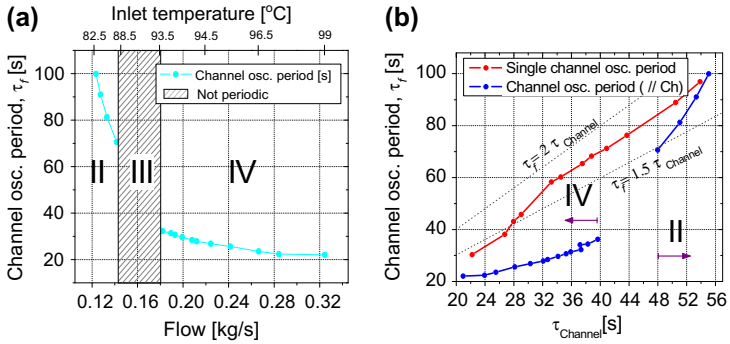

Fig. 14. (a) Period of the oscillations vs. partial flow. The a-periodical region is marked with a shaded rectangle. (b) Channel oscillation period vs. characteristic transit time in the channels for both, the single and parallel channels configuration.

[1]: the traveling time through the channel and the boiling delay time plus the bubble transit time.

Fig. 14a shows the relation between the oscillation period and the flow where the inlet temperature is included in the upper axis.

It is found that the oscillation period monotonically decreases with the inlet temperature. The figure also reveals the long incubation time from region II relative to the small oscillation period in region IV.

Fig. 14b shows the relation between the channel oscillation period and the transit time of the flow which is estimated by using Eq. (2).

The results for the single chimney configuration at equivalent conditions (in terms of the power per channel, inlet subcooling and common inlet restriction) already discussed in Section 3.1.1 are also included in the figure.

Fig. 14b clearly shows that the two regions with periodical oscillations, i.e. regions II and IV, exhibit different slopes, suggesting the instability mechanism to be different. The smaller slope of the (roughly) straight line associated with region IV is due to the strong effect of the reversed flow in the mechanism which promotes the appearance of vapor since a certain amount of hot coolant passes the heated section twice. The figure also shows that for all experiments, the parallel channels have a shorter oscillation period than that from the single chimney configuration. This difference, however, is reduced for large values of transit times, which confirms that for high subcooling/low power conditions the channels behave more independently, i.e. like in the single channel case from Section 3.1.4.

The existence of the geysering mechanism [20] which may complement flashing, is also investigated. Such a mechanism is likely to occur due to the heat transfer with the structures of the chimney section and core. The boiling delay time τ_{bd} is defined as the time required for the fluid with subcooling $\Delta T_{sub,in}$, to be heated up to the saturation temperature based on the pressure at the channel inlet and is expressed by

$$\tau_{bd} = \frac{\rho_l Cp_l \Delta T_{sub} A_C L_C}{q}, \tag{5}$$

where the liquid density ρ_l, and the specific heat capacity at constant pressure $Cp_{l,in}$, are computed at the temperature at the channel inlet; A_c and L_c are the flow area and length of the heated section, respectively.

The non-heated chimney influences the geysering period since the effect of the transport of bubbles cannot be ignored [1]. It is found an acceptable correlation for the measured data when the boiling delay time is added to the transit time of the bubbles passing through the chimney $\tau_{b,tt}$ which can be calculated by the drift velocity v_{gj}, for slug flow in the following manner

$$\tau_{b,tt} = \frac{L_{Ch}}{v_{gj} + u_{in}} \tag{6}$$

with

$$v_{gj} = 0.35\left(\frac{g\Delta\rho D_{Ch}}{\rho}\right)^{1/2}, \tag{7}$$

g being the acceleration due to gravity, $\Delta\rho$ the density difference between the liquid and vapor phases, and u_{in} the mean inlet velocity.

In experiments performed with a chimney it is reported that the period of geysering-induced oscillations τ_f, is nearly equal to the boiling delay time τ_{bd} plus the bubble transit time $\tau_{b,tt}$ [1]. The period of the oscillations τ_f are therefore plotted in Fig. 15 vs. $\tau_{bd} + \tau_{b,tt}$.

The regular oscillations from regions II and IV exhibit linear relations with different slopes. In region II the slope is roughly similar to that in the case of single channel oscillations. Since the oscillation period is several times the boiling delay time, it can be concluded that geysering plays a secondary role in this case. In contrast, the slope of the linear profile of region IV is similar to that from geysering instabilities. The magnitude of the periods, however, is systematically underpredicted, suggesting that the instability mechanism cannot be attributed to geysering only. This difference can be explained as follows. The boiling delay time assumes the flow is zero during the heating up process. The coolant flow, however, is not zero and therefore some enthalpy is transported by the coolant, which is not used in the vaporization. As a result the system needs more time to complete a cycle than that predicted by the geysering mechanism. For this reason, the period of the oscillations in region IV is overestimated by DWO based estimations and underestimated by predictions based on geysering oscillations.

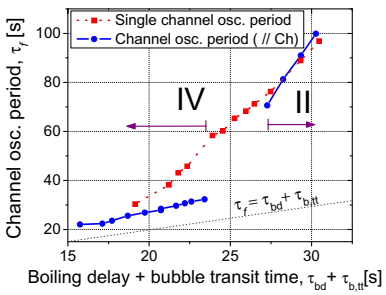

Fig. 15. Channel oscillation period vs. boiling delay time plus bubble transit time.

3.2.8. Experimental evidence of bifurcations and non-linear analysis

In this section, the experiments obtained at an input power equal to 2 kW per rod are used. The inlet temperature is varied in small steps of 0.5 °C. Each experiment is preceded by waiting 1 h before measuring, to reduce as much as possible any long term drift in the inlet subcooling. Then, each point is measured for 1 h in order to get enough statistics for this analysis.

Fig. 16a is a contour plot that shows the PSD of the primary flow signal for all measured cases. A Henning window is used. The color represents the logarithmic value of the power level for the corresponding frequency component. Fig. 16b presents the PSD for three cases.

In the out-of-phase region IV, the spectrum shows the trend of the main frequency together with higher harmonics. By decreasing the inlet temperature, a period-doubling occurs at around 96 °C. The amplitude of the successive bifurcations becomes hard to be identifiable in practice after the first period-doubling due to measurement noise.

An abrupt change in the frequency pattern is seen when reaching the a-periodical region III. Here, a broad band of frequencies emerges around the main frequency. As predicted by the Feigenbaum scenario [10], this may be due to a cascade of period-doubling bifurcations which creates many possible oscillation modes which are impossible to discriminate from each other.

In region II, the PSD clearly shows higher harmonics. A further decrease in the inlet temperature leads to the stable region I characterized by no peaks.

A non-linear characterization of experiments from region III based on a Wavelet-Transform Modulus-Maxima (WTMM) formalism showed a multi-fractal structure in the dynamics of the measured signal, thus revealing that the nature of the a-periodical oscillations is deterministic chaos [7]. As explained before, the physical mechanism driving these flow oscillations is mainly flashing combined with some geysering. Although the chaos is proven to be deterministic, such a chaotic behavior of the flow oscillations is difficult to be modelled, since there is sensitive dependence on initial conditions. Therefore, when trying to model the behavior of the facility for the transition region via a time-domain code, any inaccuracy in the determination of the initial conditions would lead to radically different responses of the facility. Any attempt to model such behaviors is further complicated by the strong asymmetrical response of each pair of heated channels/chimney.

3.3. Single channel behavior vs. two-parallel channels behavior

Table 3 shows the main features of the behaviors found for the two aforementioned configurations while the inlet temperature is increased.

First, it should be noted that the physical phenomena causing the dynamical behavior could be different for the single channel and the parallel channels configurations. A direct comparison between the behaviors a and I, b and II, etc. as stated in Table 3 is therefore not always meaningful. Second, it has to be stressed that the configurations used in both sets of experiments make use of the same loop and therefore, although the number of channels is doubled, the rest of the sections remains the same (this is different from a situation where a chimney is divided into smaller sections).

From the experiments it is observed that the stable flow circulation behavior corresponding to very low quality values in the chimney (a and I) are similar for the two configurations. This similarity can be observed in the channel axial temperature profiles, the chimney void-fraction profiles and the stable mass flow rate

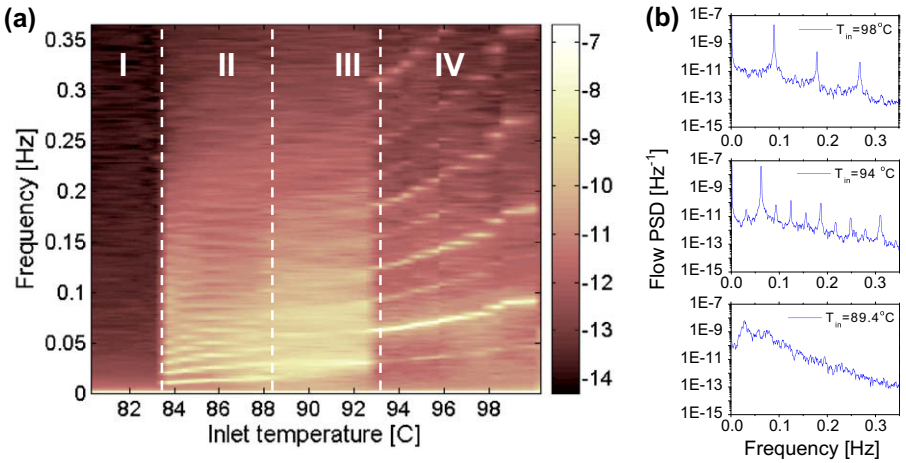

Fig. 16. (a) Contour plot of the primary flow PSD. (b) PSD for three particular cases. A bifurcation occurred from the first to the second plot.

Table 3
Summary of the different behaviors found in the experiments obtained with the single channel and the parallel channel configuration.

Single channel	Parallel channels
a – *Stable flow* mainly driven by single-phase natural circulation.	I – *Stable flow* mainly driven by single-phase natural circulation.
b – *Intermittent flow oscillations* driven by flashing. Flat chimney axial temperature profile prior to the flashing occurrence.	II – *High subcooling flow oscillations* driven by flashing and to some extent to boiling. Almost flat axial temperature profile in the chimneys prior to the flashing occurrence.
c – *Sinusoidal flow oscillations* driven by boiling plus flashing. Non-flat chimney axial temperature profile prior to the flashing occurrence.	III – *A-periodical flow oscillations* caused by flashing, boiling and geysering. Non-flat axial temperature profile in the chimneys. Reverse flow of great importance for the phenomenon.
d – *Stable flow circulation* induced by flashing.	IV – *Out-of-phase flow oscillations* driven by boiling, flashing and geysering. Non-flat chimney axial temperature profile prior to the flashing occurrence. Reverse flow of great importance for the phenomenon.

Note: The cases are ordered according to their respective inlet temperature, with cases with lower values first.

(see Figs. 4 and 10). The very high subcooling natural circulation mechanism is efficient enough to cool the heated section. Apparently the cooling mechanism is able to suppress any perturbation which would lead to instabilities in the channel(s).

The intermittent oscillations occurring in the single channel configuration show analogies to the high subcooling oscillations observed in the parallel channels configuration). This is related to the fact that flashing is the only instability – generating mechanism present here. As can be seen from Figs. 5 and 11, the axial temperature profiles are similar, except for the short time in which reverse flow occurs for the case with parallel channels. The low-quality natural circulation mechanism is not efficient enough to sufficiently cool the heating rods and reach a steady-state situation. In this case, flashing-induced instabilities and low-quality natural circulation are alternating phenomena.

The a-periodical flow oscillations involving flashing, boiling and geysering effects show a high degree of complexity and are not found in the single channel configuration. The strong coupling between the channels together with the aforementioned effects creates very complex, time-dependent, axial temperature profiles.

Some similarities exist between the sinusoidal oscillations observed in the single channel configuration and the out-of-phase oscillations in the parallel channel case (IV), such as the axial temperature profile exhibiting the same trend (see Figs. 6 and 13). The reverse flow from the latter case, however, is not present in the single channel configuration. Reverse flow shortens the flashing cycle since part of the fluid is heated twice, as can be clearly seen in Fig. 14b. The oscillation period of the partial flow in the parallel channel configuration is therefore found to be smaller than that for the single channel configuration (see Fig. 14b).

The stable flow circulation induced by flashing observed in the single channel configuration has not been found in the parallel channels cases reported here.

4. Conclusions

Flashing-induced instabilities occurring in one and two-parallel channels are investigated in detail. A novel representation of the results allowed a thorough understanding of the instability mechanism. As result of this investigation, the following is concluded.

The four different behaviors reported by previous authors are seen in the experiments obtained with the single chimney configuration: stable flow at high subcooling; intermittent flow oscillations; sinusoidal flow oscillations and stable flow at low subcooling.

The flashing front develops from the chimney top to bottom during intermittent oscillations and from bottom to top in the sinusoidal oscillations.

The oscillation period found in the experiments agrees well with those from DWOs indicating the density wave character of the flashing-induced oscillations.

The delay between the two-phase driving force and the kinetic energy is affected by the inertia of the loop.

The instability mechanisms existing when having parallel channels, have also been thoroughly investigated by using the CIRCUS test facility.

As a result of this study it is concluded that at least four different behaviors can be expected in a system of two identical heated channels equipped with parallel chimneys. These are:

- stable flow circulation (corresponding to very low vapor quality values);
- periodic oscillations in which the primary flow is roughly in-phase with the partial flow in both channels and the main instability mechanism is due to flashing. The two channels behave more or less independently except for the clear synchronization of the flashing events which can be attributed to the coupling between the channels;
- a-periodical oscillations which are attributed to multi-fractal deterministic chaos. Bifurcations have been observed in the experiments which suggest that period-doubling is the route to chaos followed by the system. This result has never been reported before; and
- out-of-phase periodical oscillations in which the primary flow exhibits a period which is half of the period of the partial flows in the channels. Two main instability mechanisms seem to coexist in this case being flashing and geysering. The channel coupling creates reversed flow which causes hot spots in the channels. This effect creates large gradients in the axial temperature profile that together with the interaction with the structures, favors the occurrence of condensation effects.

In addition, some similarities have been observed between the intermittent flow oscillations found in the single chimney experiments and the high subcooling oscillations found in the two-parallel channels experiments. Moreover, similarities have also been found between the sinusoidal flow oscillations existing in the single chimney experiments and the out-of-phase oscillations from the two-parallel channels experiments.

The results from this investigation can be very useful to validate numerical models which in turn can be used to investigate the stability of natural circulation BWRs during start-up. From the experiments with a multiple chimney configuration, it can be concluded that instabilities showing chaotic behavior might be of interest. Such a dynamical behavior may be difficult to predict by most of the time-modeling techniques, due to the sensitive dependence on initial conditions and represents a challenge for the future.

Appendix A. Supplementary material

Supplementary data associated with this article can be found, in the online version, at doi:10.1016/j.expthermflusci.2010.02.002.

References

[1] M. Aritomi, J.H. Chiang, T. Nakahashi, M. Watarum, M. Mori, Fundamental study on thermo-hydraulics during start-up in natural circulation boiling water reactors (I), J. Nucl. Sci. Technol. 29 (7) (1992) 631.
[2] M. Aritomi, J.H. Chiang, Fundamental studies on safety-related thermo-hydraulics of nat. circ. boiling parallel channel flow systems under start-up conditions (mechanism of geysering in parallel channels), accident analysis, Nucl. Safety 33 (2) (1992) 170–182.
[3] J.A. Bouré, A.E. Bergles, L. Tong, Review of two-phase flow instability, Nucl. Eng. Des. 25 (1973) 165–192.
[4] Y.K. Cheung, B.S. Shiralkar, A.S. Rao, Design evolution of natural circulation in ESBWR, in: 6th International Conference on Nuclear Engineering (ICONE-6), San Diego, USA, 1998.
[7] Ch. Demazière, C.P. Marcel, M. Rohde, T.H.J.J. Van der Hagen, Multifractal analysis of chaotic flashing-induced instabilities in boiling channels in the natural-circulation CIRCUS facility, Nucl. Sci. Eng. 158 (2) (2008) 164–193.
[9] W. De Kruijf, A. Manera, D.W. Haas, J.G.F. Schut, T.H.J.J. Van der Hagen, R.F. Mudde, Description of CIRCUS including test matrix, EC, in: 5th Euratom Framework Program 1998-2002, EVOL-NACUSP-D8a, 2001.
[10] M.J. Feigenbaum, The transition to a-periodic behavior in turbulent systems, Commun. Math. Phys. 77 (1980) 65–86.
[11] K. Fukuda, T. Kobori, Classification of two-phase flow stability by density-wave oscillation model, J. Nucl. Sci. Technol. 16 (1979) 95–108.
[12] M. Furuya, F. Inada, A. Yasuo, A study on thermalhydraulic instability of a boiling natural circulation loop with a chimney (part II. Experimental approach to clarify the flow instability in detail), Heat Transfer – Japanese Research 24 (7) (1995) 577–578.
[13] Yao. Jiang, J.H. Bo, S.R. Wo, Experimental simulation study on start-up of the 5 MW Nuclear Heating Reactor, Nucl. Eng. Des. 158 (1995) 111.
[14] J.M. Kim, S.Y. Lee, Experimental observation of flow instability in a semi-closed two-phase natural circulation loop, Nucl. Eng. Des. 196 (2000) 359–360.
[15] A. Manera, Experimental and Analytical Investigations on Flashing-Induced Instabilities in Natural Circulation Two-Phase Systems, Delft University of Technology, Delft, The Netherlands, PhD thesis, 2004.

[16] C.P. Marcel, M. Rohde, T.H.J.J. Van der Hagen, Out of- phase flashing induced instabilities in the CIRCUS facility, in: Proceedings of the 11th International Topical Meeting on Nuclear Reactor Thermal–Hydraulics (NURETH-11), Avignon, France, October 2005, pp. 1–7.
[17] C.P. Marcel, Rohde.M. Van, T.H.J.J. der Hagen, Experimental and numerical investigations on flashing-induced instabilities in a single channel, Exp. Therm. Fluid Sci. 33 (2009) 1197–1208.
[18] C.P. Marcel, Experimental, Numerical Stability Investigations on Natural Circulation Boiling Water Reactors, IOS Press, 2007 (ISBN 978-1-58603-803-8).
[20] S. Nakanishi, Recent Japanese research on two-phase flow instabilities, in: Proceedings of Japan–US Seminar on Two-phase Flow Dynamics. Hemisphere Publishing Corporation, 1979.
[21] A.S. Rao, A. Gonzalez, ESBWR program-development of passive plant technologies and designs, in: Proceedings of the Eighth International Conference on Nuclear Engineering ICONE 8205, CD-ROM Publication, 2000.
[22] A.S. Rao, A. Gonzalez, ESBWR program-development of passive plant technologies and designs, In: Proceedings of International Congress of Advanced NPPs (ICAPP), Florida, USA, vol. 1170, 2002.
[23] C. Schuster, A. Ellinger, J. Knorr, Analysis of flow instabilities at the natural circulation loop DANTON with regards to non-linear effects, Heat Mass Transfer 36 (2000) 557.
[25] E. Wissler, H.S. Isbin, N.R. Amudson, Oscillatory behavior of a two-phase natural circulation loop, AIChE J. 2 (2) (1956) 157–162.
[26] T.H.J.J. Van der Hagen, D.D.B. Van Bragt, F.J. Van der Kaa, J. Karuza, D. Killian, W.H.M. Nissen, A.J.C. Stekelenburg, J.A.A. Wouters, Exploring the Dodewaard Type-I and Type-II stability; from start-up to shut-down; from stable to unstable, Ann. Nucl. Energy 24 (8) (1997) 659–669.
[27] T. Van der Hagen, A.J.C. Stekelenburg, The low-power low-pressure flow resonance in a natural circulation boiling water reactor, Nucl. Eng. Des. 177 (1997) 229.
[28] G. Yadigaroglu, Two-phase Flow Instabilities and Propagation Phenomena, Hemisphere Publishing Corporation, 1981. pp. 353–403 (Chapter 17).